Hindawi
Advances in Civil Engineering
Volume 2020, Article ID 8825697, 10 pages
https://doi.org/10.1155/2020/8825697

Research Article

Influence of Ground Motion Parameters on the Seismic Response of an Anchored Rock Slope

Ningbo Peng,[1,2,3] **Yun Dong**,[1,3] **Ye Zhu**,[1,3] **and Jie Hong**[1]

[1]*Faculty of Architecture and Civil Engineering, Huaiyin Institute of Technology, Huaian 223001, China*
[2]*Institute for Conservation of Cultural Heritage, Shanghai University, Shanghai 200444, China*
[3]*Jiangsu Engineering Laboratory of Assembly Technology on Urban and Rural Residence Structure, Huaian 223001, China*

Correspondence should be addressed to Ye Zhu; zhuye1986@hyit.edu.cn

Received 4 June 2020; Revised 11 December 2020; Accepted 16 December 2020; Published 24 December 2020

Academic Editor: Castorina S. Vieira

The seismic response of rock slopes is closely related to the dynamic characteristics of earthquakes. In this study, based on a numerical model of rock slopes with bolt support, the seismic responses of both anchored and unanchored rock slopes under different seismic waves are calculated. The results show that a "cumulative effect" of the relative permanent displacement of the slope is generated during seismic action, and it is found that the permanent displacement of the slope is caused by larger earthquake accelerations. The dynamic responses of an anchored slope are analyzed in terms of the wave type, frequency, amplitude, and duration and are compared with those of an unanchored rock slope. This comparison suggests that the nominal shear strain increases with the amplitude and duration, which decreases as frequency increases. The axial force is directly related to the surrounding rock strain. The maximum axial force of the bolt is near the rock interface, which shows that the structural plane of the slope plays a dominant role in the seismic response. The seismic waves are random, whereas the structural plane of the rock slope is certain. The seismic response characteristics of the slope under different earthquake conditions are similar, and the dynamic stability of the slope can be attributed to the structural analysis of the rock slope.

1. Introduction

Earthquakes not only cause serious casualties and property losses, but also trigger numerous coseismic geohazards. Sliding of the slope is one of the main coseismic geohazards. Landslides are characterized by their wide distribution, large quantity, and great harm and can cause a large number of casualties and high property losses in mountainous areas [1]. For example, the Wenchuan earthquake (2008) in China triggered approximately 56,000 landslides, which caused approximately 20,000 deaths and property losses of more than 1/3 [2–4].

The stability and responses of rock slopes during earthquakes are of great concern in relation to transportation facilities and major rock engineering structures such as dams, nuclear power plants, and buildings. Due to their advantageous structure and high deformation capacity, anchor bolts are able to resist highly static and dynamic loads. In a survey of earthquake-induced geologic disasters, such as landslides and collapses, for an anchored slope, the load on the anchored structure will instantly increase at the occurrence of an earthquake [5].

Pulling tests, equations proposed by regulations, and static equilibrium equations are frequently used to determine the bearing capacity of bolts [6–8]. However, the effects of the acceleration, velocity, force duration, and frequency characteristics of vibrations that include seismic waves and blasting or mechanical vibrations have hardly been considered [9–11].

The seismic responses of anchored slopes under earthquake conditions, including the axial force of a bolt and the acceleration, velocity, and displacement of a slope caused by seismic waves [12], are the focus of recent research in the geotechnical engineering and earthquake engineering fields. Although the dynamic response of the bolt can be solved using relatively simple models, Ivanovic [13] presented a

continuous dynamic model for the axial vibration of a rock bolt system, and the results showed how the changes in the stiffness and/or length ratios affected the dynamics associated with a fixed length of the bolt and the quality of the bonding installation. Presently, only numerical analysis or experiments can be applied in studies on the seismic responses of slopes [14–17]. Ye et al. [18, 19] analyzed the seismic response of anchored slopes that included weak structural surfaces under earthquake conditions, as well as the sensitivity of bolt support parameters, and studied the failure mechanism of rock bolts by a dynamic analytical method of strength reduction. Peng and Yan [20] analyzed the seismic responses of anchored bedding rock slopes and indicated that damage to rock slopes and the axial force of bolts were related to the average tensile strain and nominal shear strain. Lin et al. [21] implemented a discrete element simulation to investigate the behavior of a dip slope under shaking table tests. The simulated dip slope model was first verified by testing under different horizontal excitations.

Clearly, under the same seismic load, the seismic responses of slopes are different according to different materials and structures. Similarly, the seismic responses are different according to the same slope under different seismic loads. The seismic response of the slope is related to the dynamic characteristics of ground motion, including the ground motion intensity, spectral characteristics, and duration time [8, 22]. The waves of an earthquake are random, and the dynamic characteristics of different seismic waves are different. Therefore, the effects of seismic parameters on the seismic response of slopes are the focus of this study.

2. Modeling

2.1. Description of Slope. Rock mass always contains some structural weakness planes, such as faults, bedding planes, fracture zones, and joints [14]. As a typical anchored rock slope model shown in Figure 1, the section structure of the anchored slope consists of layer 1 and layer 2, which are highly weathered rock and bedrock, respectively, and have a height of $H = 30$ m, a slope angle of $\theta = 60^{\circ}$, and an interfacial dip angle of $\alpha = 43^{\circ}$, as measured from the horizontal level. The mechanical properties of the rock are displayed in Table 1.

The slope is designed following the pseudostatic method, with its profile shown in Figure 1. Fully grouted rock bolts are adopted. The design parameters of the bolts are as follows: interval distance of $d = 3$ m, durep of $\beta = 20^{\circ}$, layer 2 depth of $a = 5$ m, rock bolt diameter of $r = 25$ mm, anchor hole diameter of $R = 100$ mm from bottom to top, and bolt lengths of 12 m, 11 m, 10 m, 9 m, 8 m, 7 m, and 6 m, coded from M1 to M7, respectively.

2.2. Numerical Model. The dynamic calculation is simulated by FLAC3D. The model takes 3 m in the thickness direction and is consistent with the vertical spacing of the bolt along the slope. The Mohr–Coulomb strength criterion is used as the elastoplastic material. Numerical analysis of the seismic response of surface structures such as dams requires the discretization of a region of the material adjacent to the foundation. The seismic input is normally represented by plane waves propagating upward through the underlying material. The boundary conditions at the sides of the model must account for the free-field motion that exists in the absence of the structure. These boundaries need to be placed at distances sufficient to minimize wave reflections and achieve free-field conditions. To apply the free-field boundary in FLAC3D (Figure 2), the model should be oriented such that the base is horizontal and its normal is in the direction of the z-axis, while the sides are vertical and their normal are in the direction of either the x- or y-axis.

The cable element is used to simulate the bolt. The large bonding parameters are set at the bolt anchor head to simulate the effect of the anchor head. The length of the bolt unit on each bolt is 0.5 m, and the input bolt parameters are shown in Table 2.

The boundary applies local damping, the damping coefficient is 0.15, the static calculation is carried out first, and then the dynamic calculation is carried out [23, 24]. The calculation boundary is set as follows: the distance from the slope foot to the right boundary is 1.5 times the slope height, the slope top to the left boundary distance is 2.5 times the slope height, and the upper and lower boundary heights are 2 times the slope height; these boundaries satisfy the calculation precision requirements [20]. For the convenience of the analysis of results, monitoring points are set in the model, as shown in Figure 1. The monitoring points are set along the slope surface and range from P1 to P13.

2.3. Seismic Loads. To understand the dynamic responses of rock slopes under different seismic loads, several seismic waves are input at the bottom of the slope model. The Kobe earthquake time series, El Centro earthquake time series, and cosine waves with acceleration amplitudes of 1.0 m/s^2 are selected as the basic input seismic accelerations, and the duration is 18 s, as shown in Figure 3. Seismic waves with different ground motion parameters, including wave type, amplitude, frequency, and duration, are used for calculations. With regard to the calculations, filtering and baseline adjustment techniques are used. The detailed motion parameters of all cases are shown in Table 3.

3. Result Analysis

3.1. Effect of Wave Type. Case 1 considers the effect of wave type on the seismic response of the slope. The Kobe earthquake time series, El Centro earthquake time series, and cosine waves are input at the bottom of the model, and the positive acceleration peak is 1.0 m/s^2.

3.1.1. Displacement Responses. The horizontal displacements of the anchored and unanchored slopes, at representative monitoring points P1 (slope shoulder), P8 (near the rock interface), and P12 (above the slope foot) relative to P13 (slope foot), under different types of seismic waves are shown in Figure 4. To clearly express the graphics, Kobe earthquake time series and El Centro earthquake time series

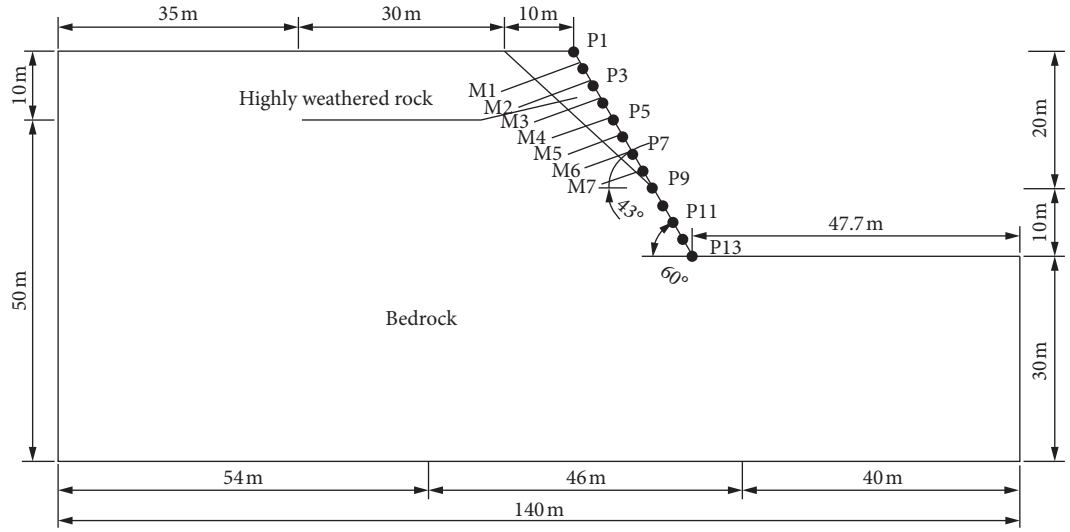

Figure 1: Modeling and monitoring points.

Table 1: Physicomechanical parameters of rock masses.

Layer	Density ($kg \cdot m^{-3}$)	Shear modulus (GPa)	Bulk modulus (GPa)	Internal friction angle (deg)	Cohesion (MPa)	Tensile strength (MPa)
1	2300	1.65	3.04	32	0.03	0.01
2	2600	10.71	7.38	47	1.00	1.60

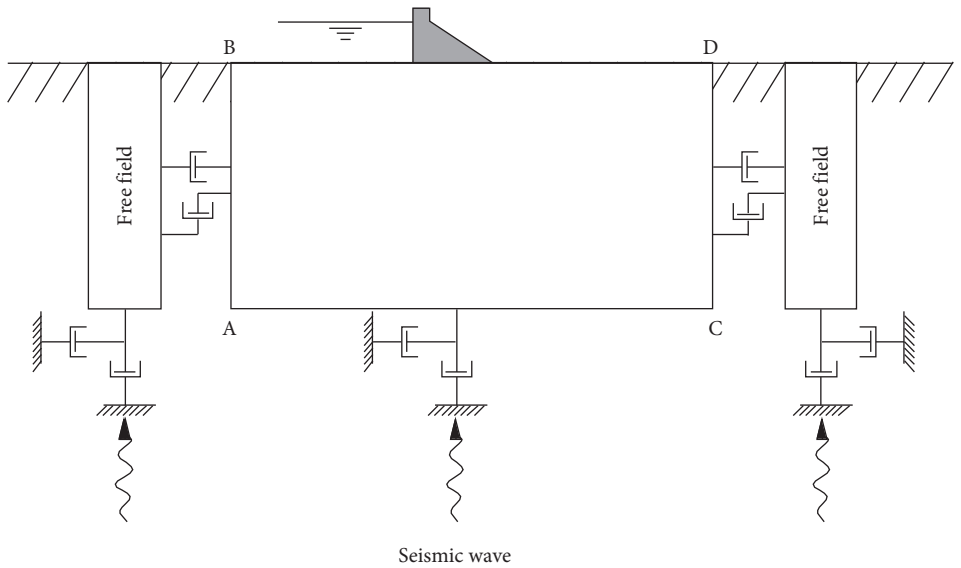

Figure 2: Model for seismic analysis of surface structures and free-field mesh.

Table 2: Mechanical parameters of the rock bolts.

Young's modulus (GPa)	Yield load (kN)	Bond stiffness ($N \cdot m^{-2}$)	Bond strength ($N \cdot m^{-1}$)	Bolt diameter (mm)	Anchor hole diameter (mm)
200	1000	1.0×10^9	2×10^8	25	100

displacement data correspond to the left Y-axis, and cosine wave displacement data correspond to the right Y-axis. This figure shows that the relative horizontal displacement of the slope is clearly different under different seismic waves. The form of the relative displacement curve is similar under the same seismic wave. The horizontal displacements under

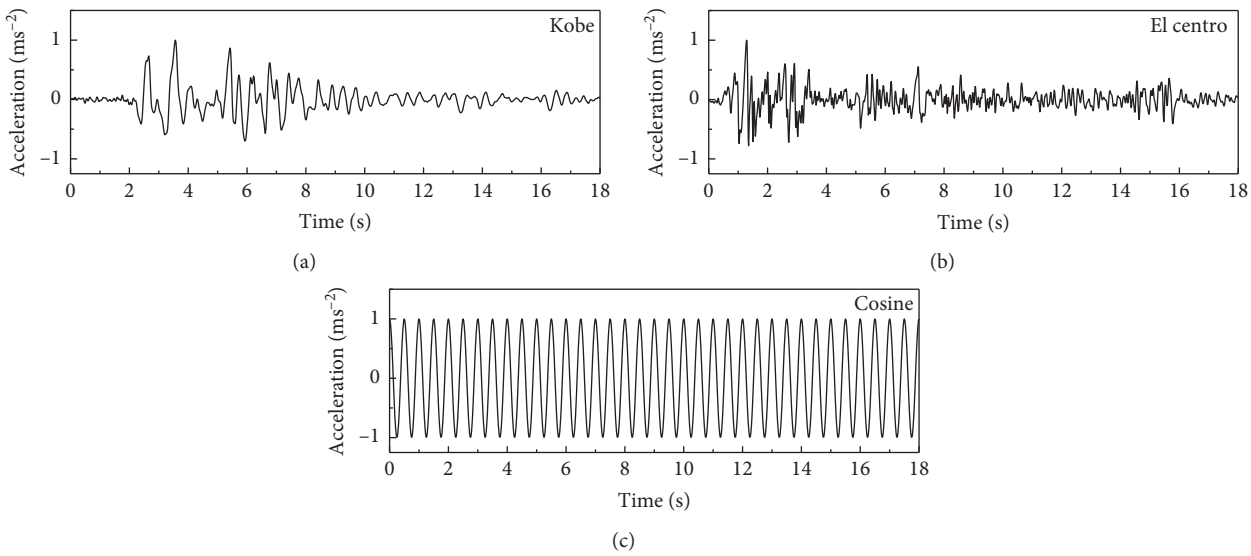

Figure 3: Input acceleration.

Table 3: Parameters of input waves under simulation conditions.

Case	Type	Amplitude (m·s^{-2})	Frequency (Hz)	Duration (s)
1–1	Kobe	1.0	1~3	18
1–2	El Centro	1.0	2~4	18
1–3/2–2/3–2/4–3	Cosine	1.0	2	18
2–1	Cosine	0.5	2	6
2–3	Cosine	1.5	2	6
3–1	Cosine	1.0	1	6
3–3	Cosine	1.0	4	6
4–1	Cosine	1.0	2	6
4–2	Cosine	1.0	2	12

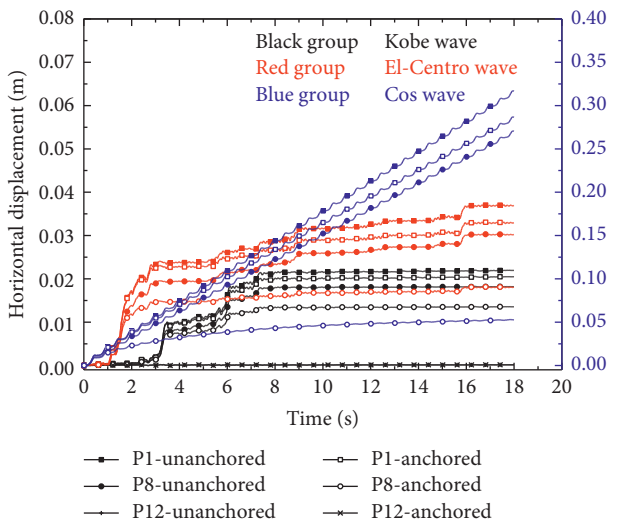

Figure 4: Relative displacement of slope with different seismic waves.

different seismic waves vary: the relative horizontal displacement of the slope under cosine waves is the highest, the El Centro earthquake time series is the second highest, and the Kobe earthquake time series is the lowest. The displacement of the anchored slope is always smaller than that of the unanchored slope, indicating that anchorage can reduce the displacement of the slope during the earthquake.

Figure 5 compares the acceleration of the Kobe and El Centro earthquake time series and the relative displacement of the slope. The permanent displacement of the slope exhibits ladder-like growth, and the Kobe seismic waves have increasingly larger accelerations than the El Centro seismic waves. Therefore, the relative displacement of the slope has more ladders with Kobe seismic waves, particularly after 8 seconds, and the permanent displacement has a greater cumulative number of times. The acceleration change in cosine waves is regular over the whole period. Therefore, the relative displacement of the slope with cosine waves increases continuously, and there is no obvious ladder-like growth. It is indicated that only sufficient acceleration can cause a permanent displacement of the slope, and the growth of the permanent displacement of the slope during the earthquake is a process with a cumulative effect. For different slopes, further study is needed to determine the acceleration threshold to stimulate permanent displacement growth.

The relative displacement of the slope directly evaluates the anchoring effect under different seismic waves, as well as

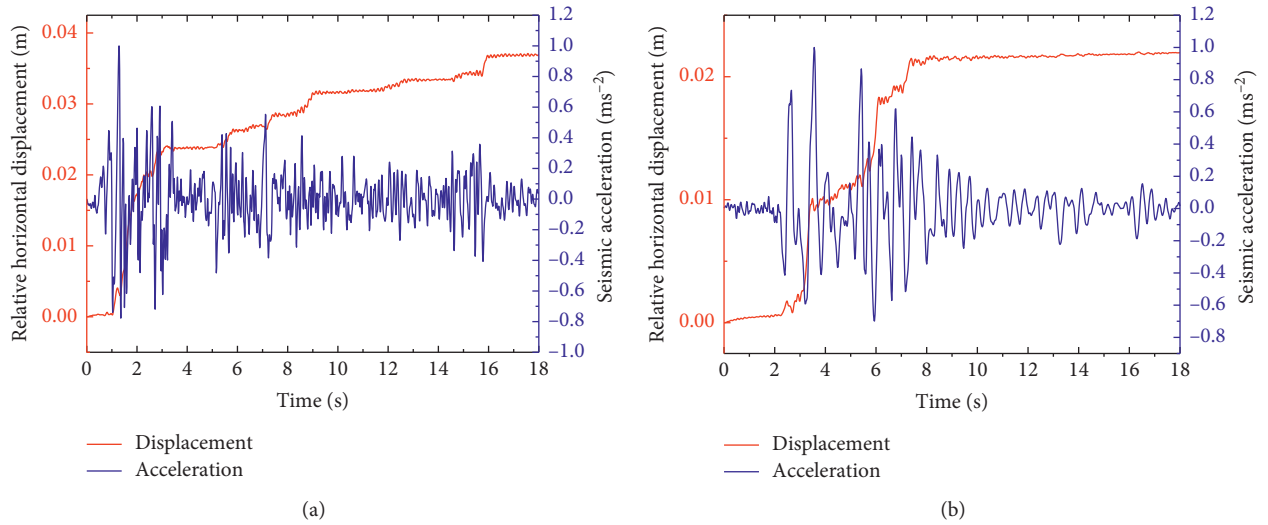

Figure 5: Cumulative effect of slope displacement. (a) Relative horizontal displacement and acceleration curves of Kobe earthquake time series. (b) Relative horizontal displacement and acceleration curves of EI Centro earthquake time series.

the nominal shear strain [20] distribution of anchored and unanchored slopes. The nominal shear strain is defined as follows:

$$\varepsilon = \frac{\Delta d_{\mathrm{xi}}}{\Delta h_i} = \frac{d_{\mathrm{xi}} - d_{x(i+1)}}{h_i - h_{i+1}}, \quad (1)$$

where d_{xi} and h_i are the horizontal displacement and elevation coordinate value of monitoring point No. i, respectively.

The nominal shear strain results are shown in Figure 6. The nominal shear strains near the slope shoulder and rock interface are relatively large under different waves, and the slope is usually destroyed in these two areas. Whether the slope is anchored or not, the nominal shear strain under cosine waves is the largest, while the El Centro earthquake time series is the second largest and that under the Kobe earthquake time series is the smallest, which is consistent with the relative horizontal displacement. The values of the maximum nominal shear strains of the unanchored slope under the Kobe earthquake time series, El Centro earthquake time series, and cosine waves are 0.007, 0.012, and 0.108, respectively, and the nominal shear strains of the corresponding anchored slope are 0.005, 0.007, and 0.021, respectively. The reductions are 28.5%, 41.6%, and 80.5%, respectively. This result illustrates that the anchoring effect of the bolt under the Kobe earthquake time series is not fully exploited, and the anchoring effect under cosine waves is the best.

3.1.2. Axial Force Responses of Bolts. Consistent with previous studies, the axial force distribution of a rock bolt exhibits a shuttle shape [25, 26], and the maximum axial force appears near the rock interface. The axial force distribution of a rock bolt is no longer attached. Figure 7 shows the maximum axial force distribution of a rock bolt in a slope under different seismic waves. The maximum axial force of the rock bolt under cosine waves is 718.2 kN, that under the El Centro earthquake time series is 188 kN, and that under the Kobe earthquake time series is the smallest at 142 kN. Thus, the larger the nominal shear strain of the slope is, the greater the axial force of the rock bolt is, and the axial force of the rock bolt is directly related to the strain of the surrounding rock.

Under the Kobe earthquake time series and El Centro earthquake time series, the higher the position of the rock bolt is, the smaller the maximum axial force is, yet the axial force distribution of the rock bolt under cosine waves does not appear regularly. This result is because the maximum nominal shear strain under cosine waves is at the position of the M2 bolt, and the potential sliding plane moves forward [8]. Thus, the rock interface is no longer on the potential sliding plane of the slope.

3.2. Effect of Amplitude. The effects of different seismic amplitudes on the dynamic response of the anchored slope are discussed in case 2 as follows. The amplitudes of seismic acceleration are 0.5 m/s^2, 1.0 m/s^2, and 1.5 m/s^2, with the same frequency of 2 Hz and a duration of 6 seconds.

3.2.1. Displacement Responses. Figure 8 shows the nominal shear strain of the slope, which shows that the distributions of nominal shear strain under different seismic waves are consistent, and the maximum nominal shear strain appears near the rock interfaces. With the increase in the amplitude of the seismic wave, the nominal shear strain of the slope increases, and the nominal shear strain of the unanchored slope is 17.1%, 58.8%, and 73.2%, indicating that the larger the amplitude is, the greater the displacement of the slope is, and the more significant the anchoring effect of the rock bolt is. Therefore, the rock bolt has less anchoring effect on the upper slope with smaller strain, yet it has a better effect on the rock interfaces with larger strain. Thus, the greater the

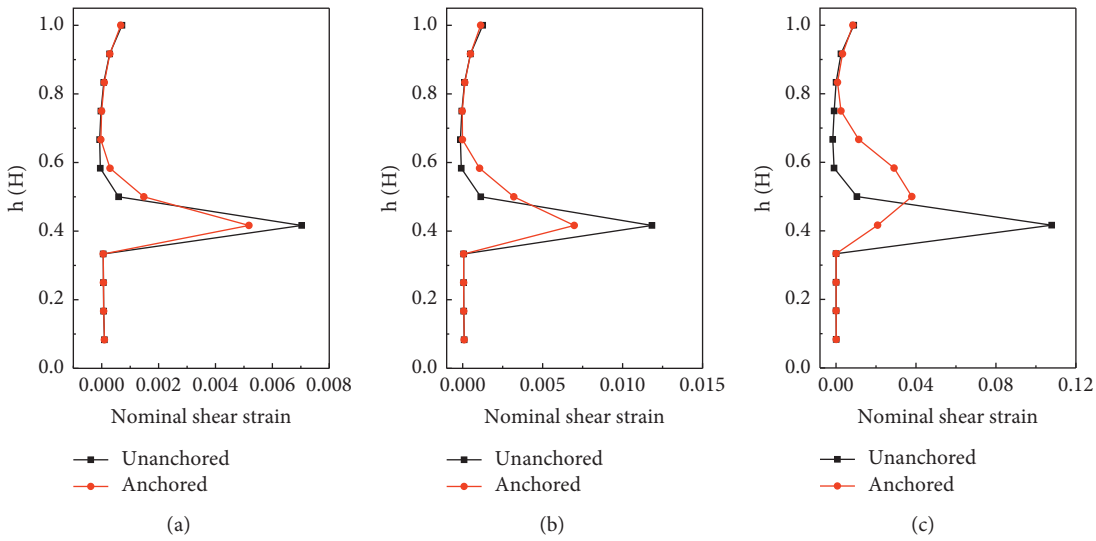

Figure 6: Nominal shear strain distribution along the elevation of the slope surface under different seismic waves: (a) the seismic wave is the Kobe earthquake time series; (b) the seismic wave is the El Centro earthquake time series; (c) the seismic wave is cosine waves.

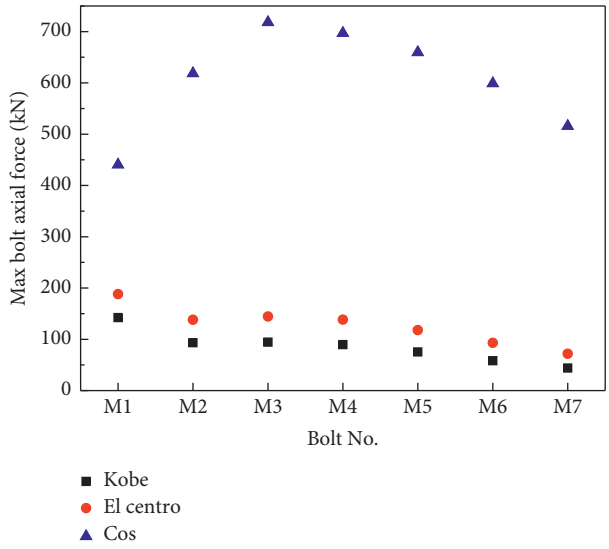

Figure 7: Maximum axial force of bolts under different types of seismic waves.

displacement of unanchored rock is, the better the anchoring effect is.

3.2.2. Axial Force Responses of Bolts. The maximum axial forces under different amplitudes under cosine waves are shown in Figure 9, which indicates that the larger the amplitude of the seismic wave is, the greater the maximum axial force is. The axial force distribution of the rock bolts exhibits a shuttle shape, and the maximum axial force appears in the rock bolt near the rock interface. The axial force of bolt M1 is the highest at an amplitude of 0.5 m/s^2, indicating that the potential slipping surface of the slope is closer to the rock interface. The axial force of bolt M1 is not the highest at an amplitude of 1.0 m/s^2, while the axial force of bolt M1 is the lowest with an amplitude of 1.5 m/s^2, indicating that the potential slipping surface moves forward under these two seismic waves. The larger the amplitude is, the greater the potential slipping surface moves forward, and the axial force is relatively smaller below the potential slipping surface.

3.3. Effect of Frequency. The dominant frequencies of real seismic waves are 1–5 Hz. To investigate the effect of different seismic wave frequencies on the seismic response of anchored slopes, we use cosine waves to calculate and analyze the following data in case 3: at frequencies of 1 Hz, 2 Hz, and 4 Hz, an amplitude of 1 m/s^2, and a duration of 6 seconds.

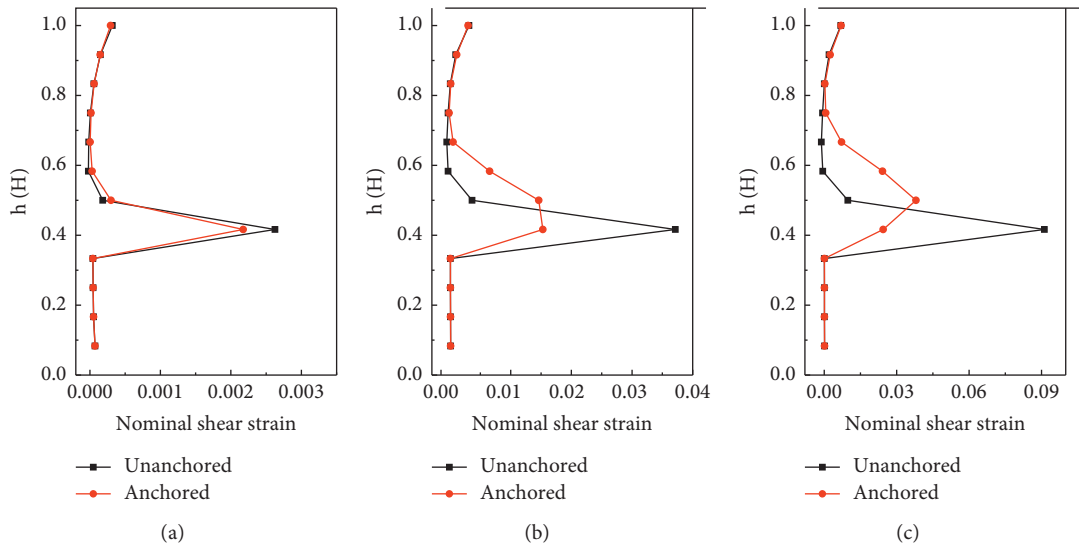

Figure 8: Nominal shear strain distribution along the elevation of the slope surface with different amplitudes: (a) amplitude is 0.5 m/s^2; (b) amplitude is 1.0 m/s^2; (c) amplitude is 1.5 m/s^2.

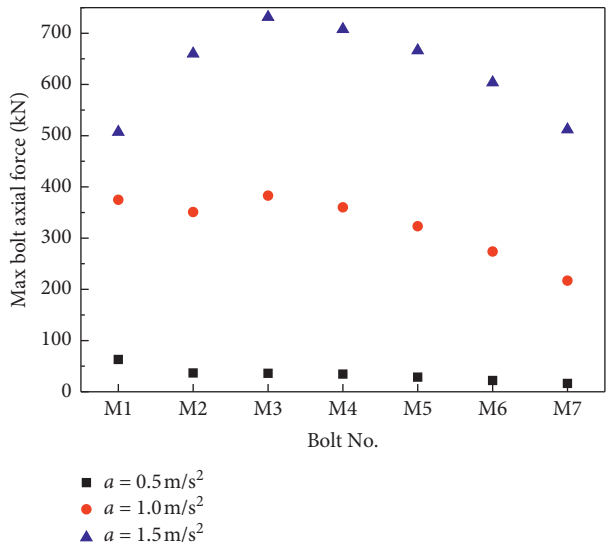

Figure 9: Maximum axial force of bolts at different amplitudes.

3.3.1. Displacement Responses. As shown in Figure 10, the results of the nominal shear strain distribution at different frequencies of cosine waves indicate that the nominal shear strain of the slope decreases with increasing seismic frequency in the ranges of the input frequency. This result is attributed to the obvious amplification effect of the rock under the low-frequency wave, and the filter effect of the high-frequency wave is strong. Furthermore, it relates to the natural vibration frequency of the rock structure. When the frequencies are 1 Hz, 2 Hz, and 4 Hz, the nominal shear strain reduction rates of the rock interface are 68.3%, 58.8%, and 56.4%, which further verifies that the greater the strain is, the better the anchoring effect of the rock bolt is.

3.3.2. Axial Force Responses of Bolts. Figure 11 shows the maximum axial force of the rock bolt in the anchored slope at different frequencies of cosine waves. With increasing seismic frequency, the maximum axial force of the rock bolt decreases. This observation indicates that, in a certain frequency range, the smaller the frequency of the earthquake is, the greater the displacement is, and the greater the axial force in the rock bolt is, the stronger the anchoring effect is.

3.4. Effect of Duration. The effect of the seismic wave duration on the seismic response of the slope is discussed in case 4 as follows. The seismic wave durations are 6 s, 12 s, and

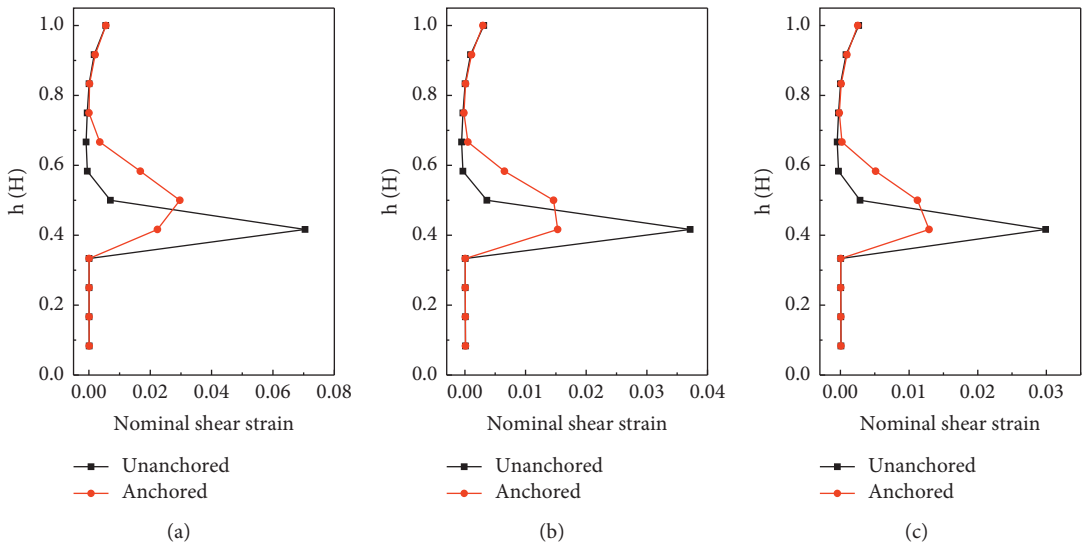

Figure 10: Nominal shear strain distribution along the elevation of the slope surface at different frequencies: (a) frequency is 1 Hz; (b) frequency is 2 Hz; (c) frequency is 4 Hz.

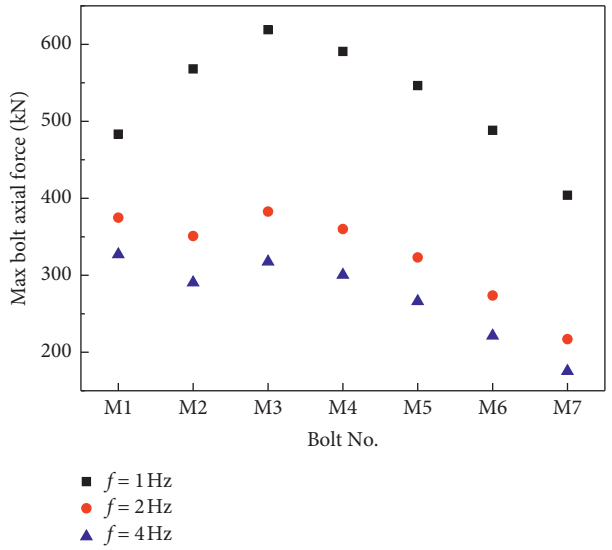

Figure 11: Maximum axial force of bolts at different frequencies.

18 s, at an amplitude of 1 m/s^2 and a frequency of 2 Hz as the input wave.

3.4.1. Displacement Responses. Figure 12 shows the nominal shear strain distribution of the slope at different durations of cosine waves. The nominal shear strain of the slope increases with the continuous input of the earthquake. The maximum nominal shear strains of the unanchored slope are 0.037, 0.073, and 0.108 for durations of 6 s, 12 s, and 18 s, respectively. The corresponding nominal shear strains of the anchored slope are 0.015, 0.019, and 0.021. The nominal shear strain reduction rates at the rock interfaces are 59.5%, 74.0%, and 80.6%. The greater the nominal shear strain is, the more obvious the anchoring effect is.

3.4.2. Axial Force Responses of Bolts. The axial forces of the bolts in the anchored slope under cosine waves for different seismic durations are shown in Figure 13. It can be seen that, with the increase in the seismic duration, the axial force of the bolt constantly increases, and the relative horizontal displacement increases as the duration increases, which further proves that the axial response of the bolt is related to the displacement response. Moreover, with increasing duration, the slope of the damage is exacerbated, the slope of

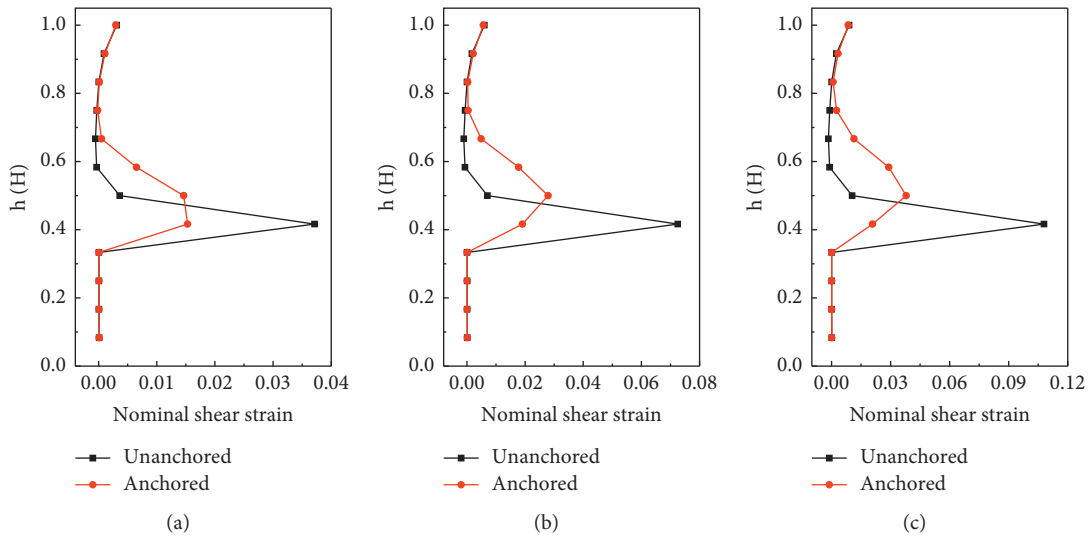

Figure 12: Nominal shear strain distribution along the elevation of the slope surface at different durations: (a) duration is 6 s; (b) duration is 12 s; (c) duration is 18 s.

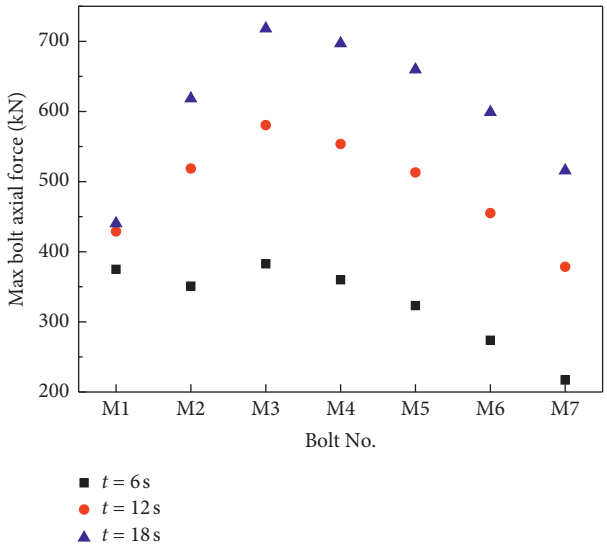

Figure 13: Maximum axial force of bolts at different durations.

the potential slipping surface moves forward, and bolt M1 is no longer the largest axial force of all the rock bolts.

4. Conclusion

The ground motion parameters are the important factors that affect the seismic responses of rock slopes. Under different seismic waves, the seismic responses of the same slope are different. To study the effects of seismic parameters on the dynamic responses of rock slopes, anchored and unanchored rock slope models were analyzed, which verify that the growth of permanent displacement is a process with a cumulative effect under a seismic effect and that permanent displacement is induced by a larger seismic acceleration. The wave type, amplitude, frequency, and duration are compared to discuss the displacement and axial force responses of the slope. The main conclusions are as follows:

First, the seismic parameters, including the wave type, amplitude, frequency, and duration, have significant effects on the seismic responses of the slope. The nominal shear strain increases with the amplitude and duration, which decreases as frequency increases. The permanent displacement of the slope is caused by a larger acceleration, and the growth of the permanent displacement of the slope during the earthquake is a process with a cumulative effect.

Second, in general, the greater the displacement response of the slope is, the greater the strain is. The greater the axial force of the bolt is, the more obvious the anchoring effects are, indicating that the axial force is directly related to the surrounding rock strain. The maximum axial force of the bolt is near the rock interface, which shows that the interface of the slope plays a dominant role in the seismic response.

Third, although the seismic responses of the slope are clearly different, there are some commonalities. The seismic response characteristics of the same slope are similar, and the rock interface is the characteristic face of the slope. The structural plane of the slope is the dominant factor of the seismic response characteristics, so the anchoring effect is mainly to change the structural characteristics of the slope. While the seismic waves are random, the structural plane of the rock slope is certain, and the displacement response characteristics of the slope are similar. Therefore, the complex dynamic problems can be greatly simplified, and the problem itself turns back to the structural characteristics of the slopes.

Data Availability

All relevant data underlying in this research was included in this paper.

Conflicts of Interest

The authors declare that they have no conflicts of interest.

Acknowledgments

The authors acknowledge the support of the National Natural Science Foundation of China (Nos. 51808246 and 51808247), the National Key Research and Development Program of China (No. 2019YFC1520500), the Natural Science Foundation of the Jiangsu Higher Education Institutions of China (No. 17KJA560001), the Six Talent Peaks Project in Jiangsu Province of China (No. JZ-011), the Open Fund of State Key Laboratory of Coastal and Offshore Engineering (No. LP1829), and the Open Fund of Jiangsu Engineering Laboratory of Assembly Technology on Urban and Rural Residence Structure (Nos. JSZP201901 and JSZP201902).

References

[1] H. S. Liu, J. S. Bo, and D. D. Liu, "Review on study of seismic stability analysis of rock-soil slopes," *Earthquake Engineering and Engineering Vibration*, vol. 25, no. 1, pp. 164–171, 2005.

[2] T. Gorum, X. Fan, C. J. van Westen et al., "Distribution pattern of earthquake-induced landslides triggered by the 12 May 2008 Wenchuan Earthquake," *Geomorphology*, vol. 133, no. 3-4, pp. 152–167, 2011.

[3] R. Huang and X. Fan, "The landslide story," *Nature Geoscience*, vol. 6, no. 5, pp. 325-326, 2013.

[4] Y. P. Yin, "Researches on the geo-hazards triggered by Wenchuan earthquake, Sichuan," *Journal of Engineering Geology*, vol. 16, no. 4, pp. 433–444, 2008.

[5] S. Sun, J. Wang, and J. Zheng, "Analysis of a railway embankment landslide induced by the Wenchuan earthquake, China," *Soil Mechanics and Foundation Engineering*, vol. 50, no. 2, pp. 56–60, 2013.

[6] S. K. Shukla and M. M. Hossain, "Stability analysis of multi-directional anchored rock slope subjected to surcharge and seismic loads," *Soil Dynamics and Earthquake Engineering*, vol. 31, no. 5-6, pp. 841–844, 2011.

[7] S. Shukla and M. Hossain, "Analytical expression for factor of safety of an anchored rock slope against plane failure," *International Journal of Geotechnical Engineering*, vol. 5, no. 2, pp. 181–187, 2011.

[8] Y. R. Zheng, H. L. Ye, R. Q. Huang, A. H. Li, and J. B. Xu, "Study on the seismic stability analysis of a slope," *Journal of Earthquake Engineering and Engineering Vibration*, vol. 30, no. 2, pp. 173–180, 2010.

[9] M. G. Iskander, J. Liu, and S. Sadek, "Transparent amorphous silica to model clay," *Journal of Geotechnical and Geoenvironmental Engineering*, vol. 128, no. 3, pp. 262–273, 2002.

[10] L. B. Martin, M. Tijani, F. Hadj-Hassen, and A. Noiret, "Assessment of the bolt-grout interface behaviour of fully grouted rock bolts from laboratory experiments under axial loads," *International Journal of Rock Mechanics and Mining Sciences*, vol. 63, pp. 50–61, 2013.

[11] T. J. Siller, P. P. Christiano, and J. Bielak, "Seismic response of tied-back retaining walls," *Earthquake Engineering and Structural Dynamics*, vol. 20, no. 7, pp. 605–620, 1991.

[12] G. X. Xu, L. K. Yao, Z. H. Li, and Z. N. Gao, "Dynamic response of slopes under earthquakes and influence of ground motion parameters," *Chinese Journal of Geotechnical Engineering*, vol. 30, no. 6, pp. 918–923, 2008.

[13] A. Ivanovic and R. D. Neilson, "Influence of geometry and material properties on the axial vibration of a rock bolt," *International Journal of Rock Mechanics & Mining Sciences*, vol. 45, no. 6, pp. 941–951, 2008.

[14] O. Aydan, Y. Takahashi, N. Iwata, R. Kiyota, and K. Adachi, "Dynamic response and stability of un-reinforced and reinforced rock slopes against planar sliding subjected to ground shaking," *Journal of Earthquake and Tsunami*, vol. 12, no. 4, p. 1841001, 2018.

[15] J. Song, Y. Gao, T. Feng, and G. Xu, "Effect of site condition below slip surface on prediction of equivalent seismic loading parameters and sliding displacement," *Engineering Geology*, vol. 242, pp. 169–183, 2018.

[16] J. Wang, J. Liu, Q. Liang, and X. Ouyang, "Dynamic response to seismic waves at the shallow slope supported by bolts," *Geotechnical and Geological Engineering*, vol. 36, no. 4, pp. 1991–2001, 2018.

[17] M. Xu, Y. Tang, X. Liu, H. Yang, and B. Luo, "A shaking table model test on a rock slope anchored with adaptive anchor cables," *International Journal of Rock Mechanics and Mining Sciences*, vol. 112, pp. 201–208, 2018.

[18] H. L. Ye, Y. R. Zheng, R. Q. Huang, A. H. Li, and X. L. Du, "Analysis on dynamic response of rock bolt in rock slope under earthquake," *Journal of Logistical Engineering University*, vol. 26, no. 4, pp. 1–7, 2010.

[19] H. L. Ye, Y. R. Zheng, R. Q. Huang, X. L. Du, and A. H. Li, "Sensitivity analysis of parameters for bolts in rock slopes under earthquakes," *Chinese Journal of Geotechnical Engineering*, vol. 32, no. 9, pp. 1374–1379, 2010.

[20] N. B. Peng and Z. X. Yan, "Dynamic responses of anchored rock slope under earthquake – a numerical study," *Disaster Advances*, vol. 6, no. 2, pp. 4–11, 2013.

[21] C.-H. Lin, H.-H. Li, and M.-C. Weng, "Discrete element simulation of the dynamic response of a dip slope under shaking table tests," *Engineering Geology*, vol. 243, pp. 168–180, 2018.

[22] S. W. Qi, "Two patterns of dynamic responses of single-free-surface slopes and their threshold height," *Chinese Journal of Geophysics*, vol. 49, no. 2, pp. 518–523, 2006.

[23] Itasca Consulting Group Inc, *FLAC3D Version 4.0 (Fast Lagrangian Analysis of Continua in 3 Dimensions) User's Manual*, Itasca Consulting Group Inc, Minnepolis, MN, USA, 2009.

[24] M. Manica, E. Ovando, and E. Botero, "Assessment of damping models in FLAC," *Computers and Geotechnics*, vol. 59, pp. 12–20, 2014.

[25] Y. Cai, T. Esaki, and Y. Jiang, "A rock bolt and rock mass interaction model," *International Journal of Rock Mechanics and Mining Sciences*, vol. 41, no. 7, pp. 1055–1067, 2004.

[26] C. A. You, "Analysis of bond-type bolt stress with overall length," *Chinese Journal of Rock Mechaics and Engineering*, vol. 19, no. 3, pp. 339–341, 2000.